Electromagnetic Particle-in-Cell Model with AMR and Application to Current Sheet Evolution in 2D and 3D Systems

Keizo Fujimoto

宇宙科学セミナー＠NiCT

on December 3, 2007

Introduction

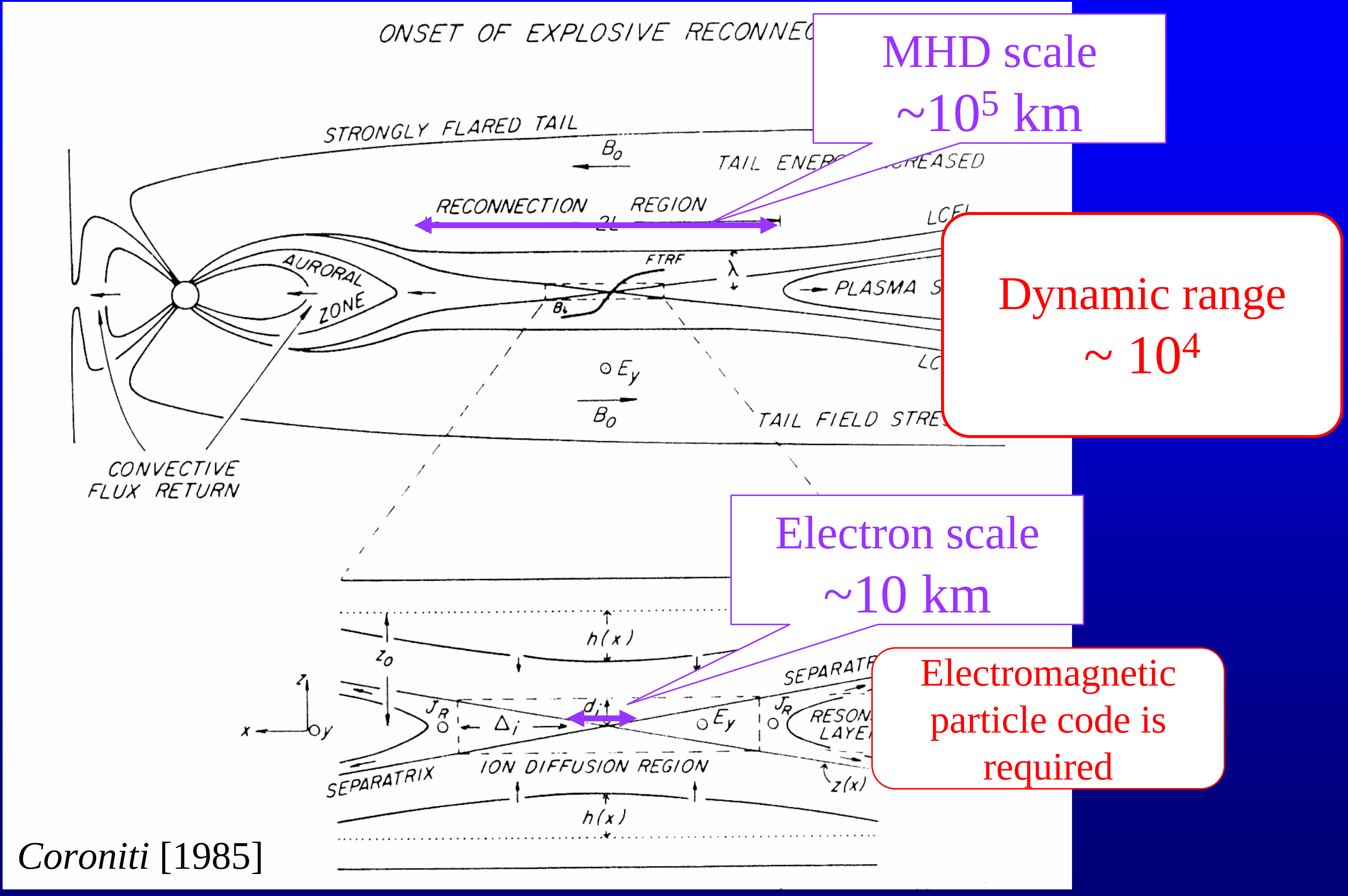

Coroniti [1985]

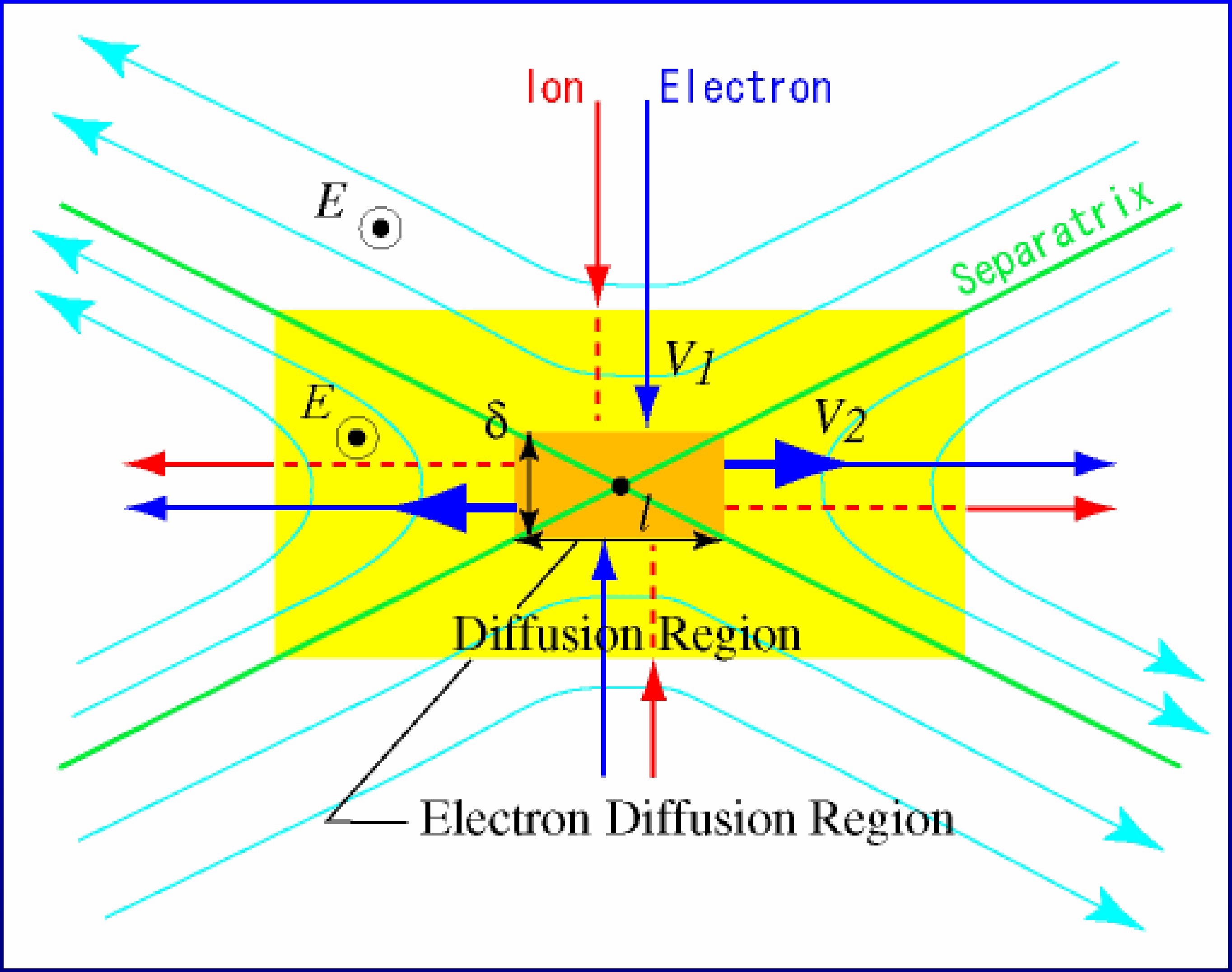
Ion
Electron
E
Separatrix
V1
E
δ
V2
l
Diffusion Region
Electron Diffusion Region

Introduction

Restriction in full particle code: $\Delta x \lesssim 3\lambda_{De} \sim 1km$

[*Birdsall & Langdon*, 1995]

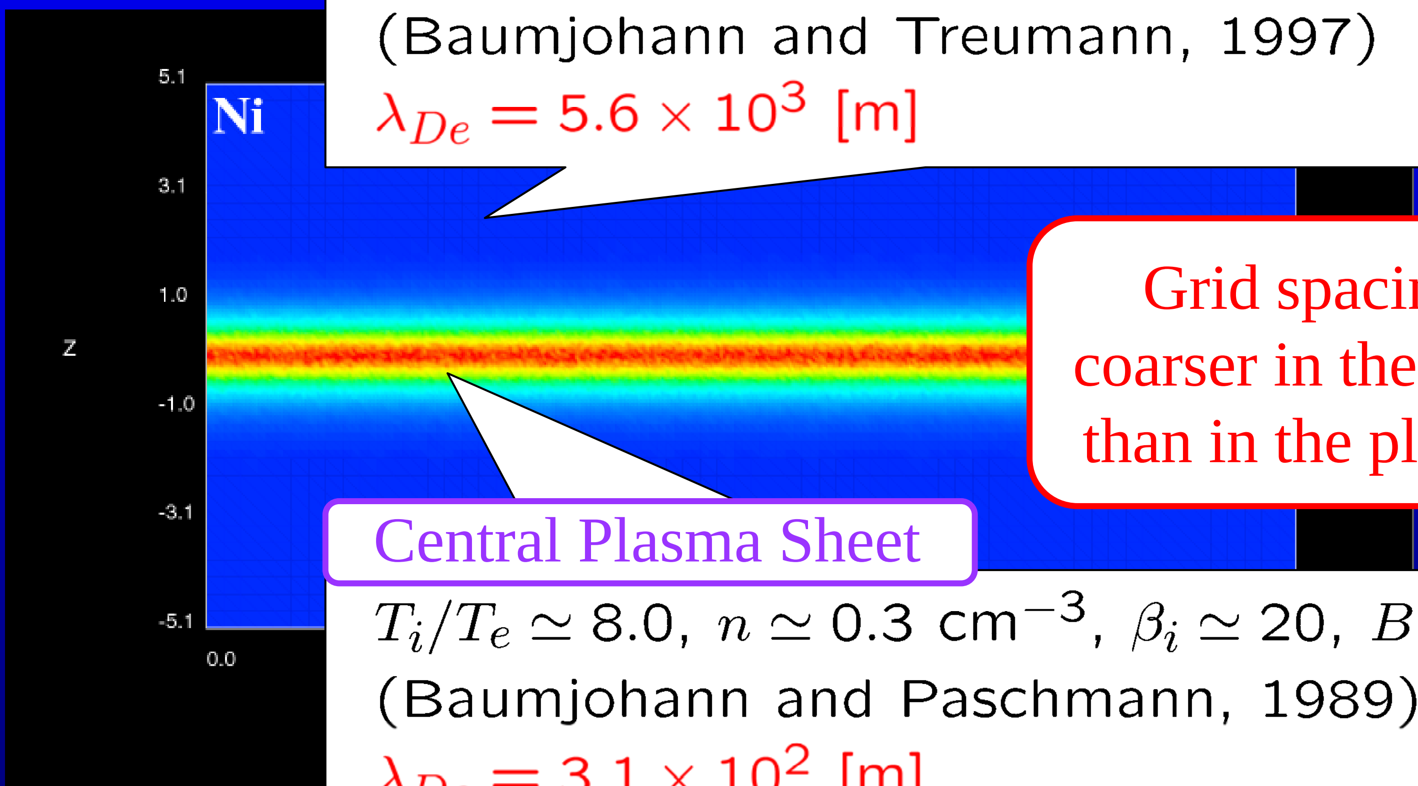

Magnetotail Lobe

$T_i/T_e \simeq 4.0$, $n \simeq 0.01$ cm^{-3}, $\beta_i \simeq 0.1$, $B = 30$ nT.
(Baumjohann and Treumann, 1997)
$\lambda_{De} = 5.6 \times 10^3$ [m]

Grid spacing can be coarser in the lobe region than in the plasma sheet.

Central Plasma Sheet

$T_i/T_e \simeq 8.0$, $n \simeq 0.3$ cm^{-3}, $\beta_i \simeq 20$, $B = 5$ nT.
(Baumjohann and Paschmann, 1989)
$\lambda_{De} = 3.1 \times 10^2$ [m]

Introduction

Restriction in full particle code: $\Delta x \lesssim 3\lambda_{De} \sim 1km$

[*Birdsall & Langdon*, 1995]

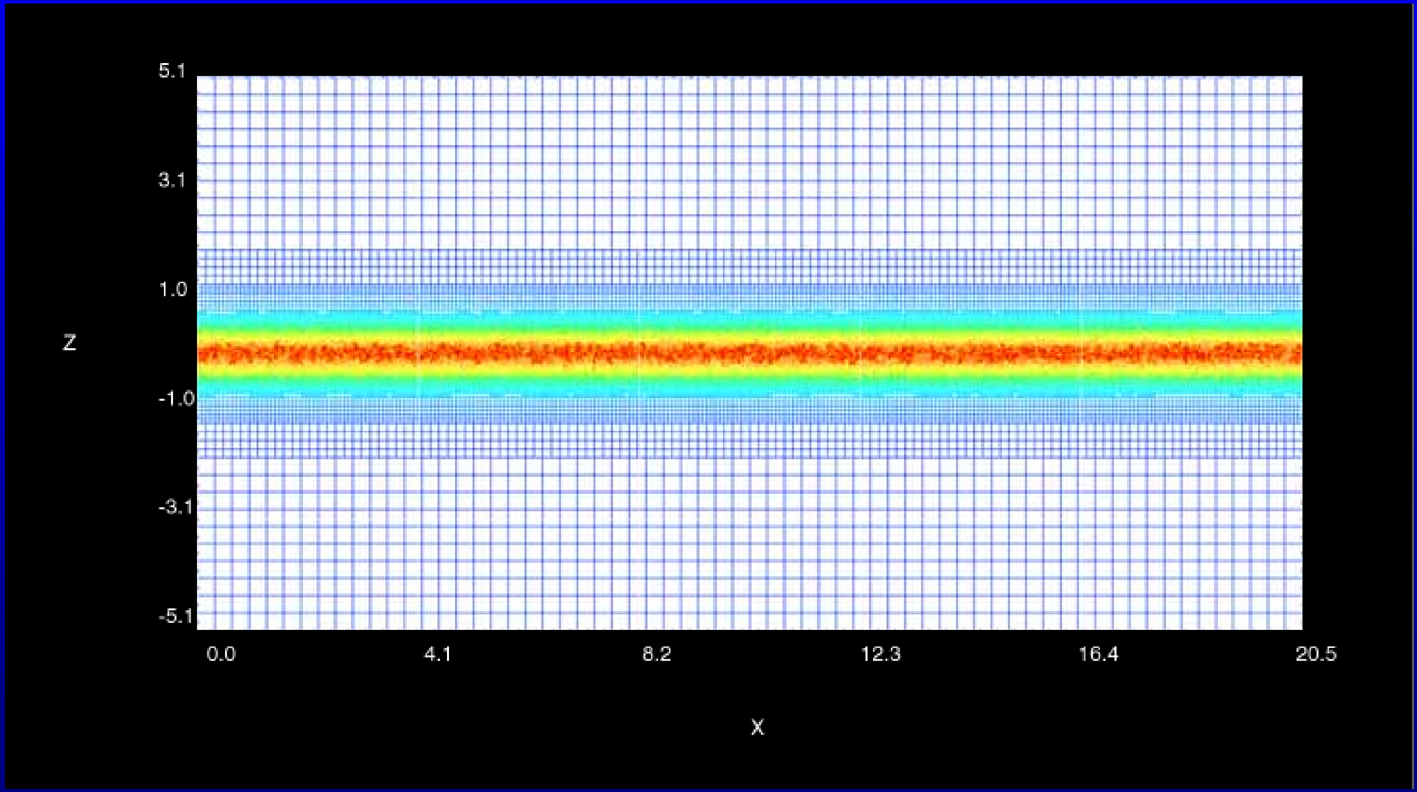

AMR法の使用例

✓ **多階層格子を偏微分方程式系に適用**

Berger and Oliger (1984), Berger and Colella (1989)

✓ MHD + AMR

Groth et al. (2000)

✓ PIC + AMR (N-body code)

Villumsen (1989), Jessop et al. (1994), Suisalu and Saar (1995), Gelato et al. (1997), Kravtsov et al. (1997), Yahagi and Yoshii (2001)

✓ EMPIC + AMR

Fujimoto and Machida (2006)

Data Structure

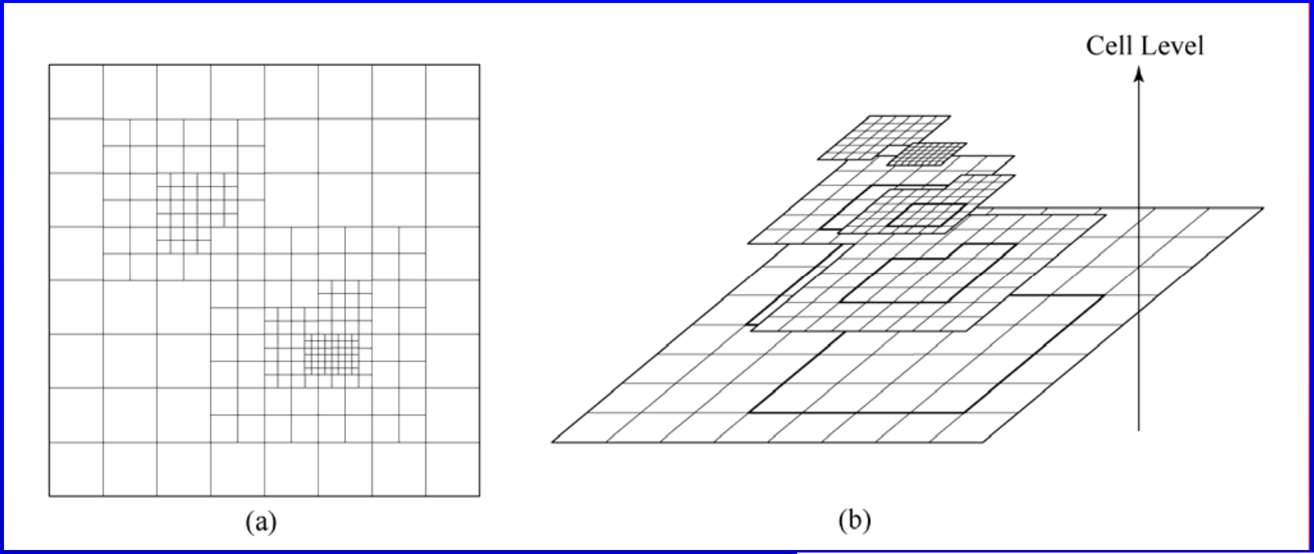

Cells are treated as independent units organized in refinement trees rather than elements of arrays, so that a very flexible cell hierarchy is achieved.

The hierarchical cell structure is supported by a set of pointers, which is basically same as the fully threaded tree (FTT) structure [*Khokhlov*, 1989].

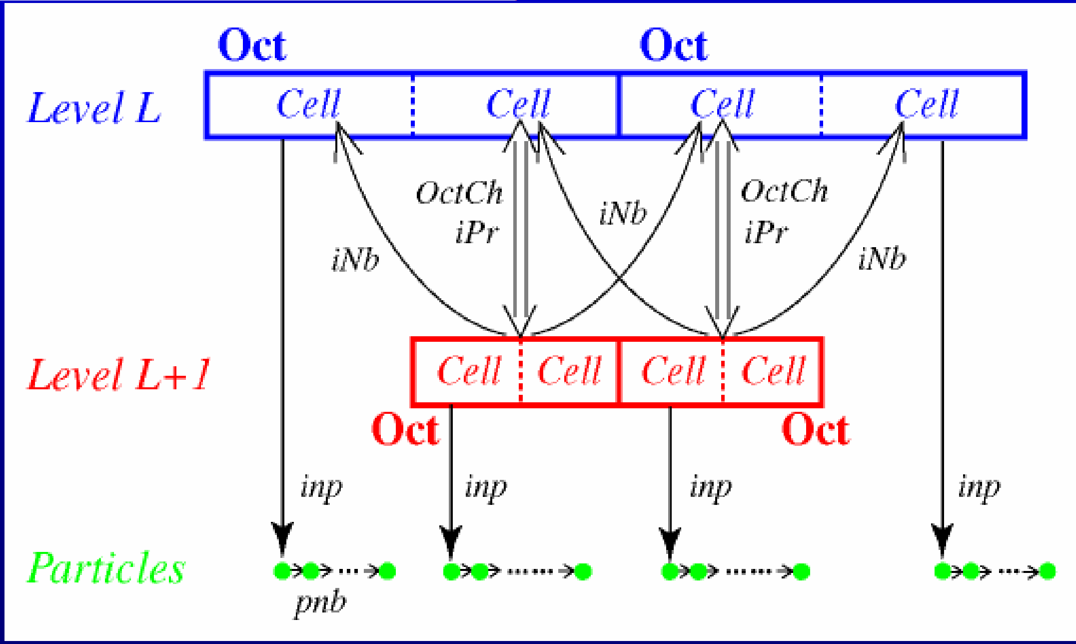

Basic Equations

- Equation of motion

$$\frac{d\boldsymbol{x}_s}{dt} = \boldsymbol{v}_s, \quad \frac{d\boldsymbol{v}_s}{dt} = \frac{q_s}{m_s}[\boldsymbol{E}(\boldsymbol{x}_s) + \boldsymbol{v}_s \times \boldsymbol{B}(\boldsymbol{x}_s)] \quad (s = i,\, e)$$

- Electromagnetic field

$$\boldsymbol{E} = \boldsymbol{E}_L + \boldsymbol{E}_T \quad (\nabla \times \boldsymbol{E}_L = 0, \nabla \cdot \boldsymbol{E}_T = 0),$$

$$\boldsymbol{E}_L = -\nabla\phi, \qquad \nabla^2\phi = -\rho/\varepsilon_0,$$

$$\frac{\partial \boldsymbol{E}_T}{\partial t} = c^2\nabla \times \boldsymbol{B} - \boldsymbol{j}_T/\varepsilon_0 \qquad (\boldsymbol{j}_T = \boldsymbol{j} + \nabla\eta),$$

$$\frac{\partial \boldsymbol{B}}{\partial t} = -\nabla \times \boldsymbol{E}_T$$

$$\eta = -\varepsilon_0\frac{\partial\phi}{\partial t} \qquad \text{(Charge continuity equation)}.$$

Calculation of Electromagnetic Field

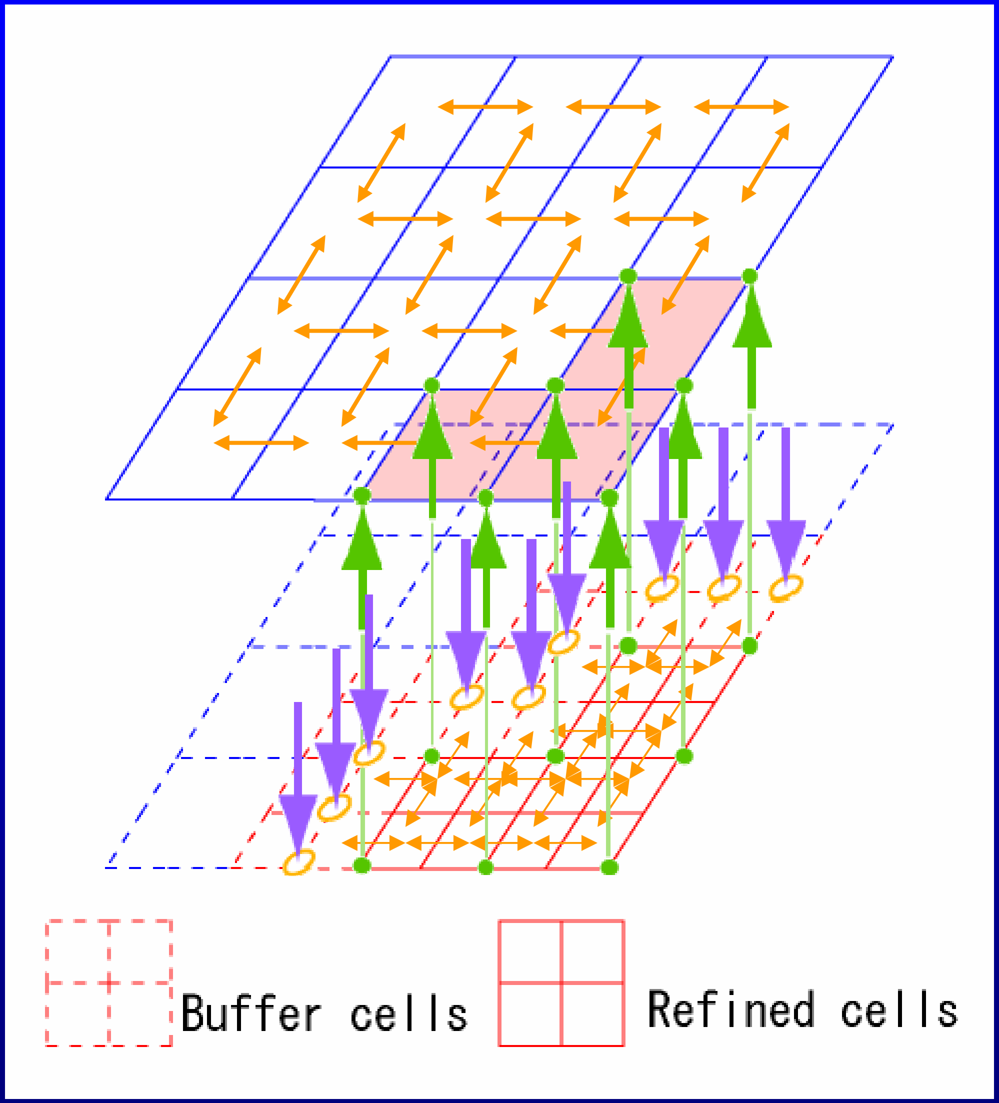

EM solver on the coarsest cells

Interpolation to the buffer cells

EM solver on the finer cells

Projection of the solution on the finer cells onto the coarsest cells

Mesh Refinement Criteria

Electron Debye length alone is really enough?

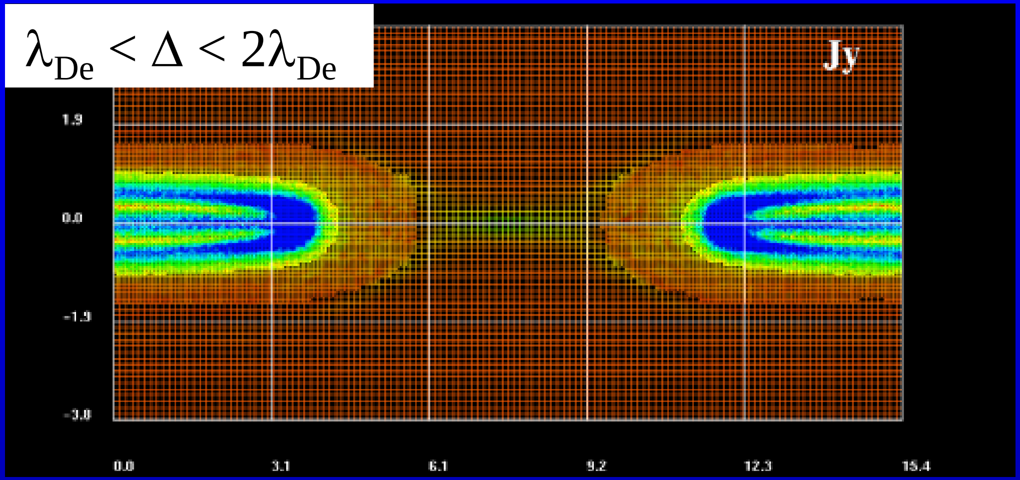

Aliasing

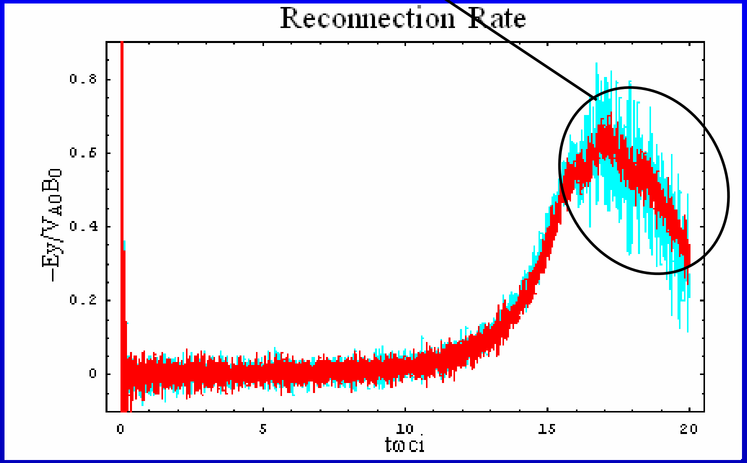

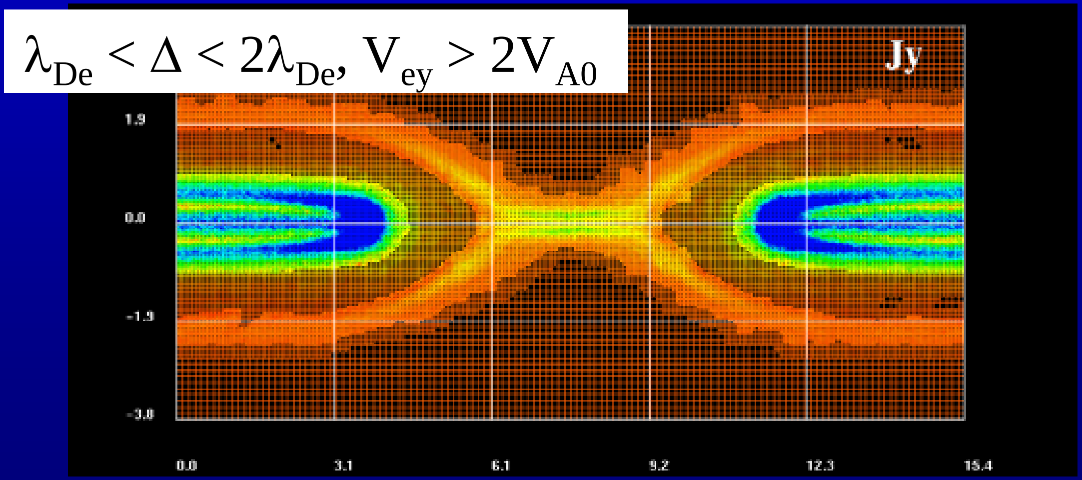

Refinement meshes are required in the region where the electron scale physics is expected to be significant.

The Number of Meshes and Simulation Cost

- The number of meshes

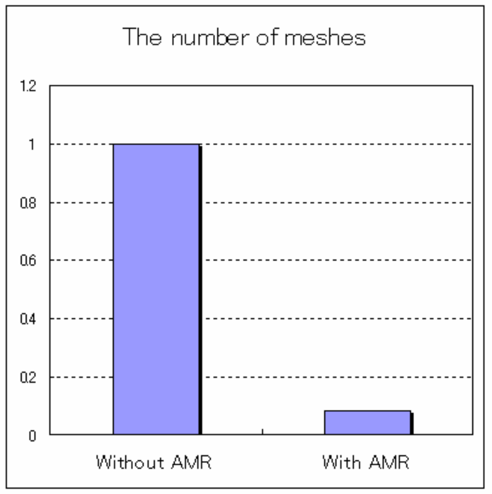

- Walltime

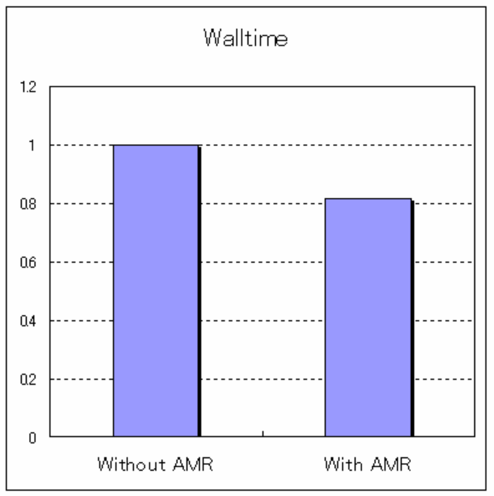

- Simulation cost

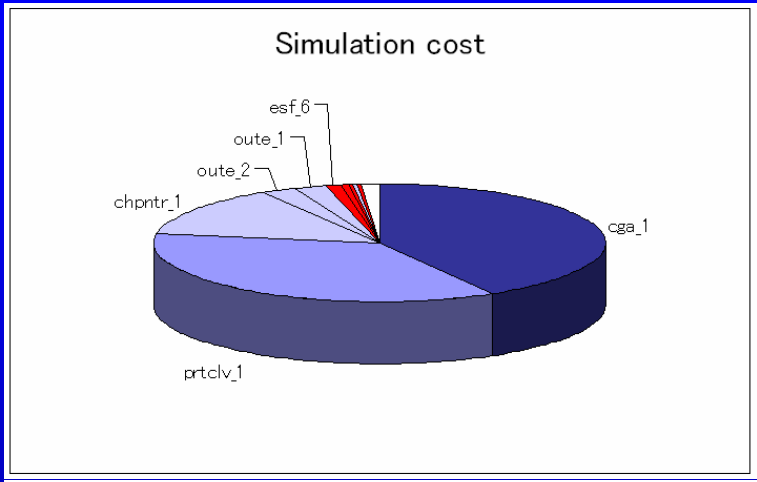

96 % of the total simulation time is devoted to the routines related to the particle data.

In order to perform an efficient simulation, it is inevitable to reduce the number of superparticles.

Particle Splitting and Coalescence (Lapenta, 2002)

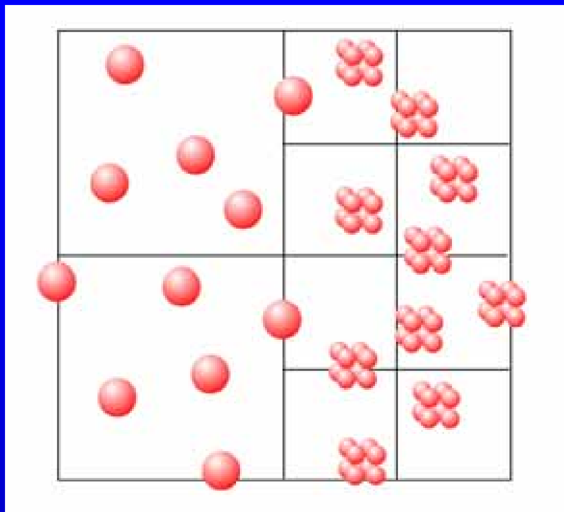

$$\frac{d\vec{v}_s}{dt} = \boxed{\frac{q_s}{m_s}} \left(\vec{E} + \vec{v}_s \times \vec{B} \right)$$

Conserving through the splitting

Moment on the grids (ρ_c, J), Total charge and mass ($\Sigma\rho_c$, Σm), Total energy of particles ($\Sigma mv^2/2$), Distribution function (f(v))

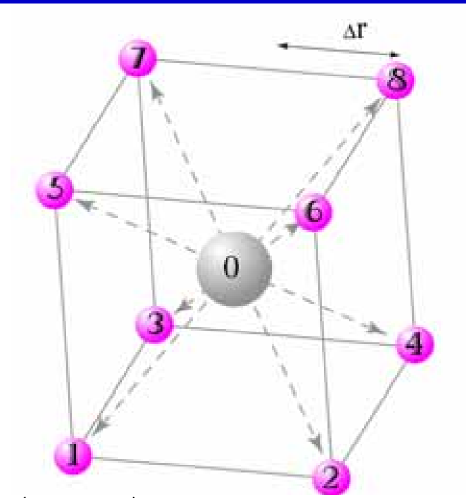

$$\vec{v}_i = \vec{v}_0$$
$$q_i = q_0/8,\ m_i = m_0/8$$
$$i = 1, 2, \ldots, 8$$

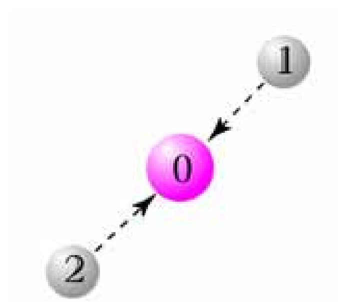

$$q_1 = q_2;\ m_1 = m_2$$
$$\vec{x}_0 = (\vec{x}_1 + \vec{x}_2)/2$$
$$\vec{v}_0 = (\vec{v}_1 + \vec{v}_2)/2$$
$$q_0 = q_1 + q_2$$
$$m_0 = m_1 + m_2$$

- Wall time

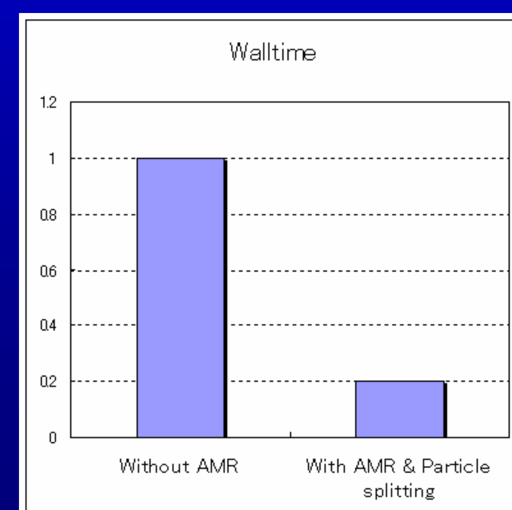

Initial Setting for the Test Simulations

Harris-type current sheet

$B_x(z) = B_0 \tanh[z/\lambda]$

$J_y(z) = J_0 \, \mathrm{sech}^2[z/\lambda]$

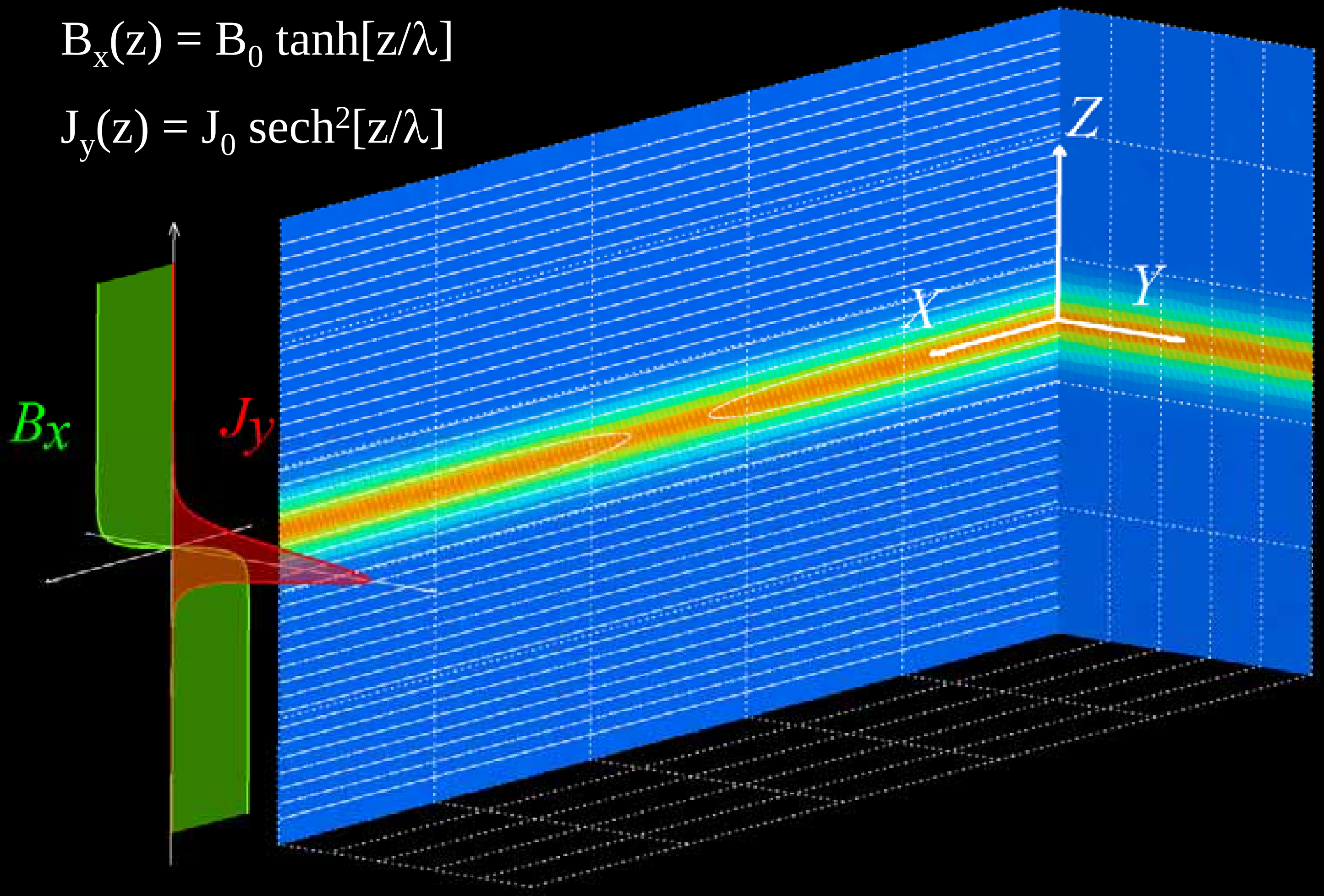

Test Simulations in the Non-tearing System

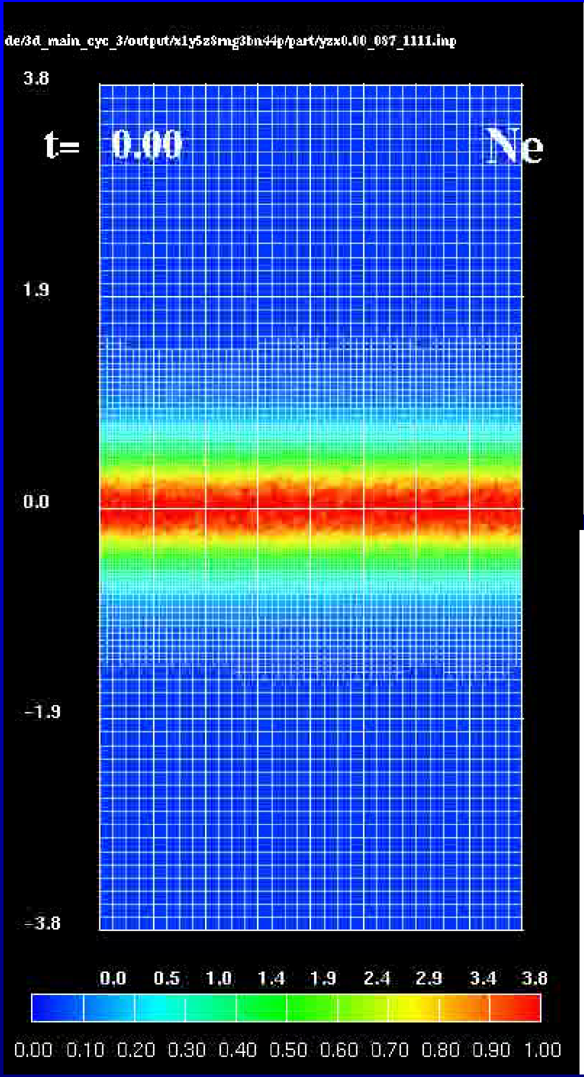

Linear dispersion of the lower hybrid drift instability

$$1+\frac{\omega_{pe}^2}{\omega_{ce}^2}\left(1+\frac{\omega_{pe}^2}{c^2k^2}\right)-\frac{2\omega_{pi}^2}{k^2v_i^2}\left(1+\frac{\beta_i}{2}\right)\frac{kV_i}{\omega-kV_e}$$
$$+\frac{2\omega_{pi}^2}{k^2v_i^2}\left[1+\xi Z(\xi)\right]=0$$
$$\xi=(\omega-kV_i)/kv_i$$

[*Davidson et al.*, 1977]

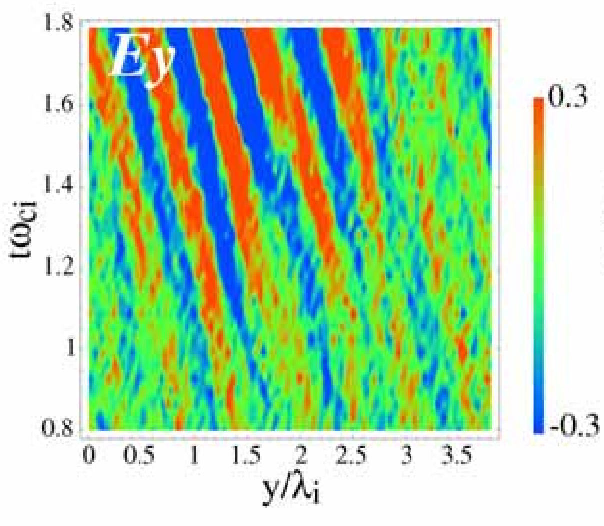

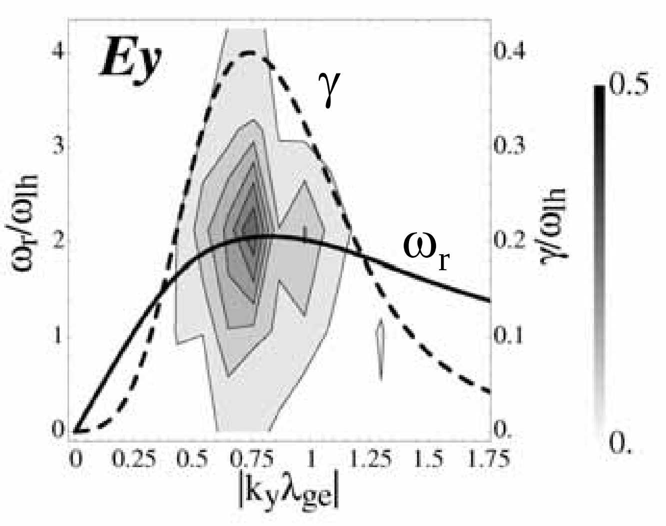

Test Simulations on Magnetic Reconnection

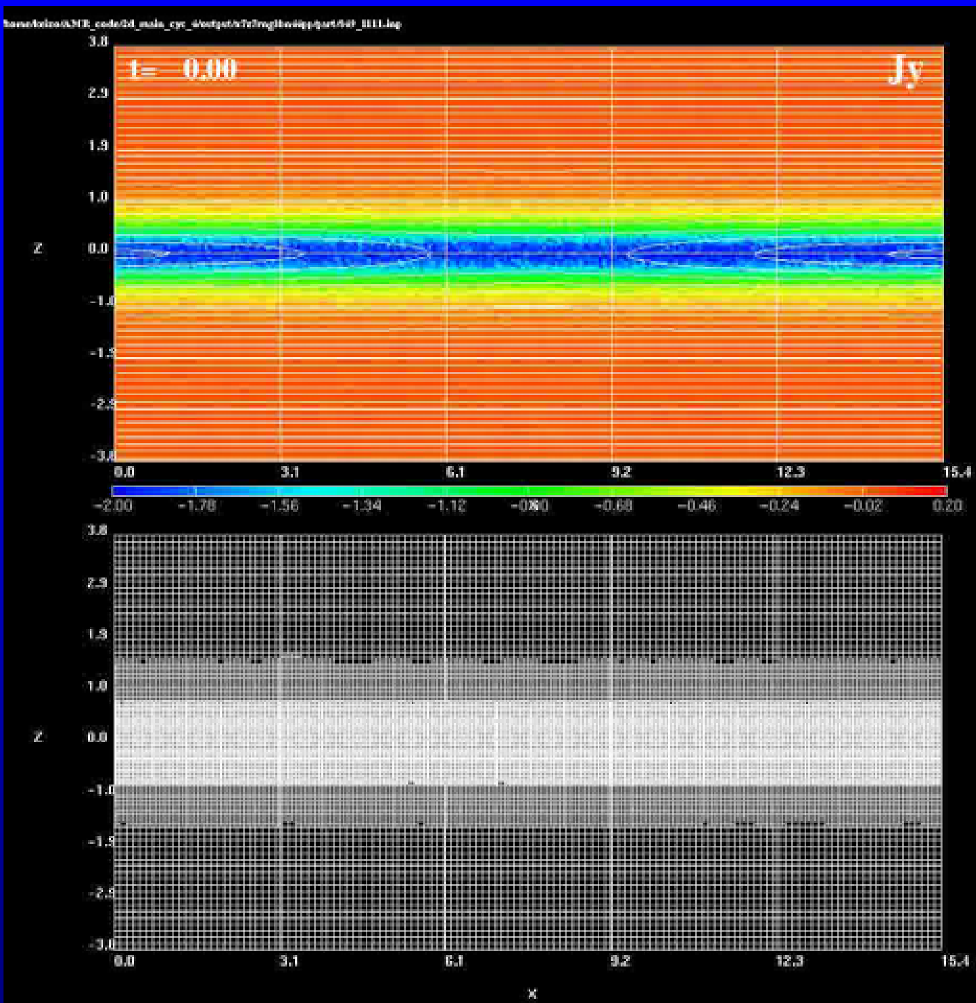

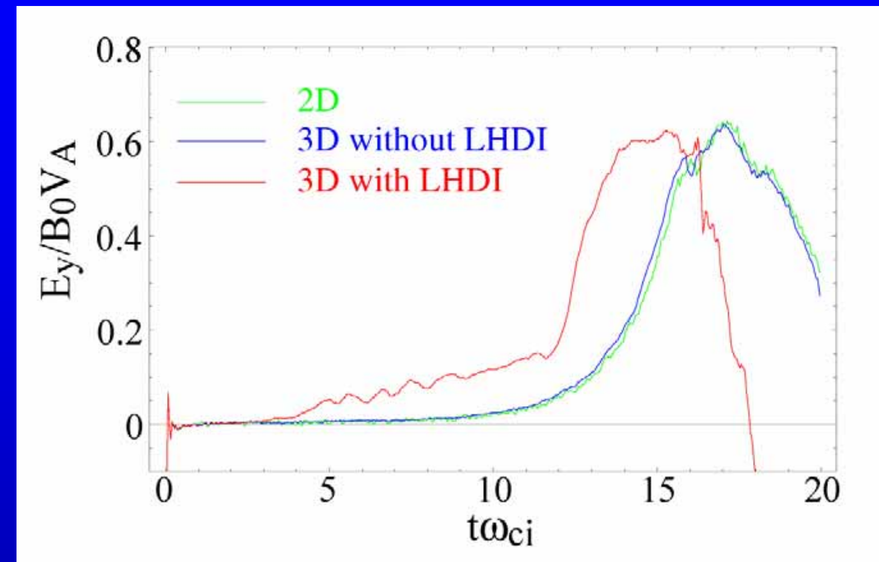

In 3D system with the lower hybrid drift instability (LHDI), the current density is enhanced at the center of the current sheet, which facilitates the onset of a fast reconnection.

Tearing and Kink Modes in 3D System

System size: $L_x \times L_y \times L_z = 30.7\lambda_i \times 7.7\lambda_i \times 30.7\lambda_i$

Maximum resolution: $N_x \times N_y \times N_z = 1024 \times 256 \times 1024$

$m_i/m_e = 25$

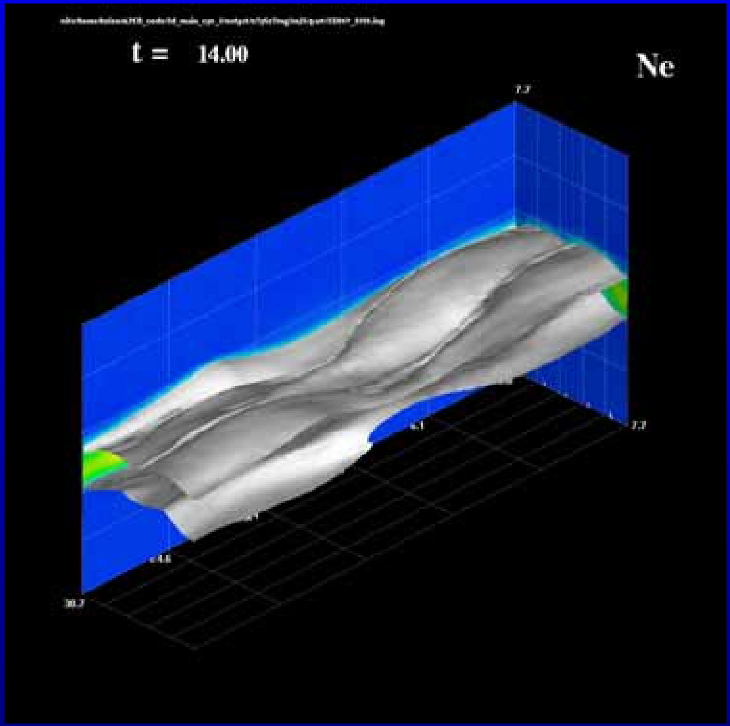

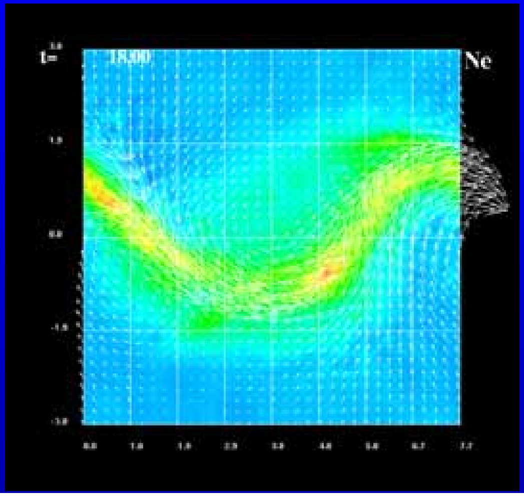

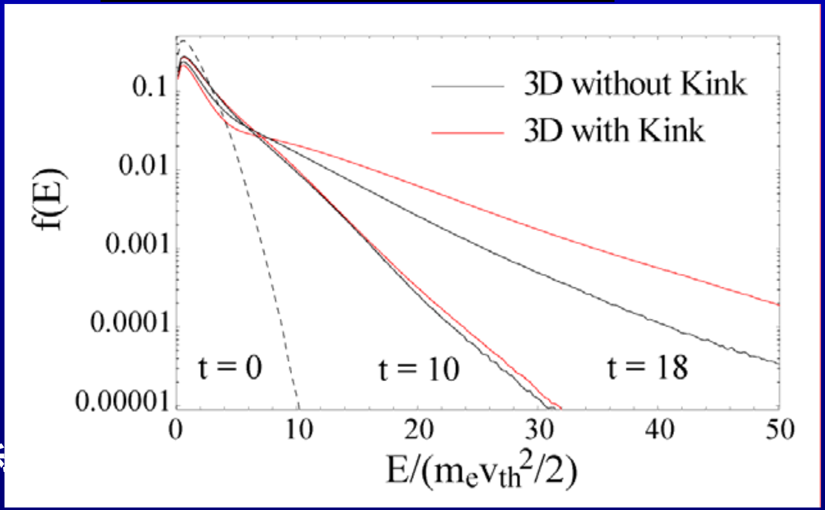

Parallelization Efficiency

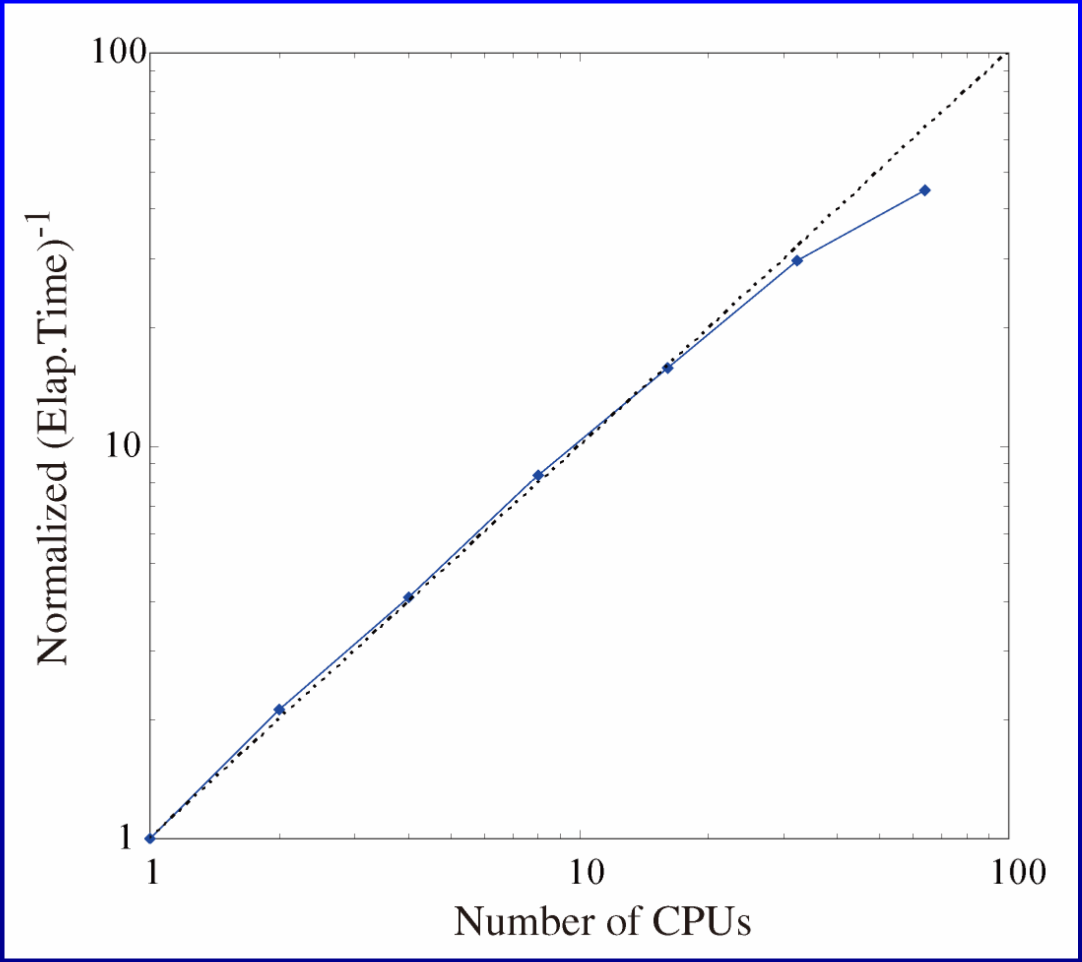

(The test was performed using the FUJITSU HPC2500.)

Summary and Conclusions

We have successfully developed new 2D and 3D electromagnetic particle code with the adaptive mesh refinement technique.

- Refinement meshes are required not only in the region with small Debye length, but also in the region where the electron scale physics is expected to be significant.
- In order to perform an efficient simulation, it is inevitable to reduce not only the number of meshes, but also the number of superparticles.
- Numerical errors associated with cell refinement and particle coalescence are small.
- The code is checked against the LHDI and Tearing instability.
- The computing performance and efficiency are well enhanced by parallelizing the code, using the OpenMP and MPI.